5 Mathematical process model

The industrial scale production of highly pure oxygen and nitrogen as well as noble gases is still carried out by means of the cryogenic process.

The initial process for production of pure oxygen first developed by Carl von Linde and first operated by Linde in 1902 [3] consisted of only a stripping section, in a way only half a rectification column. The reason for that is while it is easy to supply the heat necessary for the reboiler, a heat sink to operate a condenser at temperatures of about $95\ K$ is not readily available on our planet. due to that highly pure oxygen could be withdrawn from the bottom of the column, but nitrogen was only produces at mediocre purities.

The breakthrough that enabled operation of a "full" column, again developed by Linde in 1910, was to operate the column sections at different pressures. That way the energy needed in the reboiler could be withdrawn from the condenser of the other column half. This leads to a somewhat inverted construction of the tower in comparison to regular distillation units, because the lower section forms the top section in this case and condenser and reboiler usually at the top and bottom of a column are combined in a single heat exchange unit in the middle of the column. This specialty of the process also leads to the need that the absolute values of the energies used in condenser and reboiler need to be equal. On terms of modelling the process this also forms a considerable challenge.

A simplified overview of the major process steps is given in fig. 5.1. Within the following sections the different process steps will be discussed in more detail. When appropriate the mathematical model for single process units is discussed as well. In addition to the separate process steps displayed in fig. 5.1 the aspect of heat integration os essential to successfully operating an air separation unit (ASU). This aspect will be discussed separately as well (sec. 5.3)

The pre-purification step of the process aim to reduce the amount of unwanted impurities from the ambient air as far as possible. The main sources of contamination are in this case dust and other organic components that can be found depending on the time of year and location of the plant. Furthermore are water and carbon dioxide common components in ambient air. The removal of these components is undertaken by means of adsorption molecular sieves such as zeolite or for initial steps coarser sieves. However the design and simulation of these pre-purification measures is not within the scope of this work. For more information the interested reader is referred to [1].
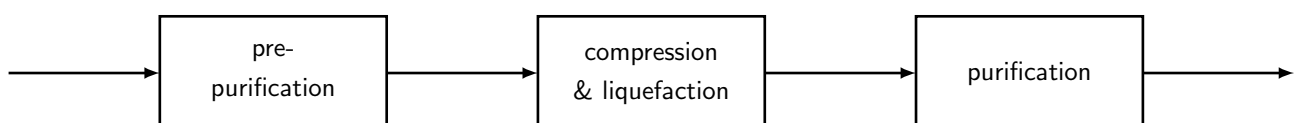

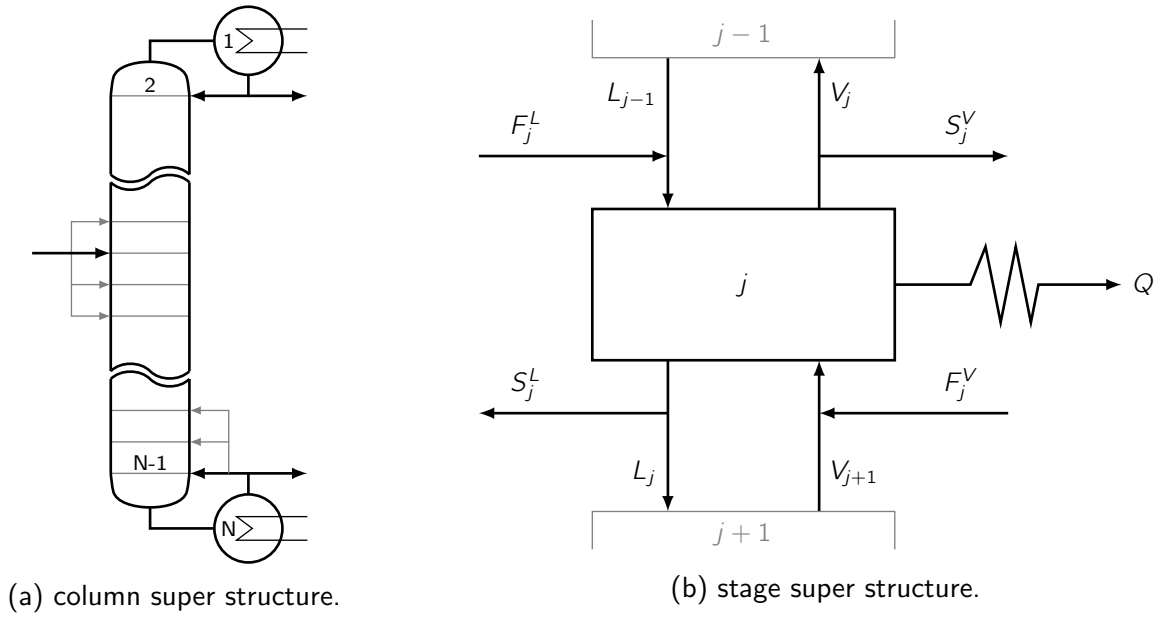Figure 5.1: simplified cryogenic air separation process.

(a) column super structure.

(b) stage super structure.

Figure 5.2: superstructures for column and column stages.

5.1 Purification

The purification of the liquefied gases is performed by distillation columns operated at different pressure. These distillation columns form the heart of the air separation process and their operation parameters are crucial in terms of enabling the desired separation. While the aspect of heat integration poses is also essential in terms of profitability of the process.

Subsequently this section is concerned with the description of different aspects of modeling distillation columns. First the mathematical model will be presented in more detail. Afterwards the handling of different specifications for individual columns is elaborated upon. Lastly the issue of initializing the respective models and the implemented solution is presented.

5.1.1 Distillation column model

In this section the working equations used to model the different distillation columns in the process, known as the MESH equations, are given. These equations, although rather plain at first glimpse, form a set of highly non-linear, highly coupled equations. The solutions of these equations is not a trivial task for current solution algorithms, whose success is highly dependent on the quality of initial guesses provided. Therefore a strategy used for the automated generation of such guesses will be described as well.

Fig. 5.2a and fig. 5.2b show the super structures for a distillation column with a single feed and and no side draws and an inner column stage. The acronym MESH stands for Material (M), Equilibrium (E), Summation (S) and Enthalpy (H) equations which are given below.

Material balances The material balances in their most general form for an inner column stage can be written as

$$0 = \left(V_j + S_j^V\right) \cdot y_{i,j} + \left(L_j + S_j^L\right) \cdot x_{i,j} - V_{j+1} \cdot y_{i,j+1} - L_{j-1} \cdot x_{i,j-1}$$
$$- F_j^V \cdot z_{i,j}^V - F_j^L \cdot z_{i,j}^L, \qquad i = 1 \ldots C, \quad j = 1 \ldots N. \quad (5.1)$$

Here the vapour and liquid phase of the feed to the stage are considered separately. While this is not strictly necessary is allows for certain freedoms in terms of modelling column operations, as sometimes the vapour fraction of a given feed is actually fed into the vapour phase of a stage and therefore effectively in the liquid phase of the stage above.

To facilitate convergence the side draw streams S_j^V and S_j^L are made dimensionless by means of the respective vapour and liquid flows on that stage to form the vapour

$$s_j^V = \frac{S_j^V}{V_j}, \qquad j = 1 \ldots N \qquad (5.2)$$

and liquid

$$s_j^L = \frac{S_j^L}{L_j}, \qquad j = 1 \ldots N \qquad (5.3)$$

stripping factors. Replacing the side-streams in the material balances by their corresponding stripping factors yields

$$0 = \left(1 + s_j^V\right) \cdot V_j \cdot y_{i,j} + \left(1 + s_j^L\right) \cdot L_j \cdot x_{i,j} - V_{j+1} \cdot y_{i,j+1} - L_{j-1} \cdot x_{i,j-1}$$
$$- F_j^V \cdot z_{i,j}^V - F_j^L \cdot z_{i,j}^L, \qquad i = 1 \ldots C, \quad j = 1 \ldots N. \quad (5.4)$$

As the model is also to be used for optimization purposes further extensions are necessary. The location of individual feeds as well as the number of theoretical or real stages of the column is to be optimized. To accommodate that need, new variables need, namely the feed split ζ_{ij}^F for feed i to stage j as employed by [9] are introduced. The split variables are integer variables that can take a value of 0 or 1. Additionally it is assumed that each feed will only be fed to a single stage thus

$$0 = 1 - \sum_{j=1}^{N} \zeta_{ij}, \qquad i = 1 \ldots F, \quad j = 1 \ldots N, \qquad (5.5)$$

where F denotes the number of feeds, comprised of vapour (F^V) and liquid F^L feeds.

In order to optimize the number of stages several superstructures are possible. One can optimize the reboiler reflux location and condenser reflux location or each single one along with the feed and side draw locations. The stage number is then changed as all stages between condenser or reboiler reflux are effectively rendered inactive. The solution of the mass and energy balances for each respective stages becomes trivial as only one single vapour or liquid stream enters and exits the stage. While

the choice if condenser and or reboiler reflux is optimized is somewhat arbitrary some studies have shown [11] that the strategy of optimizing only feed location and reboiler reflux location possesses some numerical advantages in terms of performance of the solution algorithm.

With the newly introduced split variables for liquid ζ_{ij}^L and vapour ζ_{ij}^V as well as the reboiler reflux ζ_j^R and the liquid ζ_{ij}^{SL} and vapour ζ_{ij}^{SV} side draws, the material balances can be written as

$$0 = \left(1 + s_j^V\right) \cdot V_j \cdot y_{i,j} + \left(1 + s_j^L\right) \cdot L_j \cdot x_{i,j} - V_{j+1} \cdot y_{i,j+1}$$

$$- L_{j-1} \cdot x_{i,j-1} - \sum_{k=1}^{F^V} \zeta_{kj} \cdot F_j^V \cdot z_{i,j}^V - \sum_{l=1}^{F^L} \zeta_{lj} \cdot F_j^L \cdot z_{i,j}^L - \zeta_j^R \cdot V_N \cdot y_{iN},$$

$$i = 1 \ldots C, \quad j = 1 \ldots N, \quad k = 1 \ldots F^V, \quad l = 1 \ldots F^L. \quad (5.6)$$

Furthermore to be able to optimize side draws, the stripping factors have to be reformulated accordingly

$$s_j^V = \frac{\sum_{i=1}^{S^V} \zeta_{ij}^{SV} S_j^V}{V_j}, \qquad j = 1 \ldots N, \quad i = 1 \ldots S^V, \tag{5.7}$$

$$s_j^V = \frac{\sum_{i=1}^{S^L} \zeta_{ij}^{SL} S_j^L}{L_j}, \qquad j = 1 \ldots N, \quad i = 1 \ldots S^L. \tag{5.8}$$

Equilibrium equations   The equilibrium equations are given by

$$y_{ij} = K_{ij} \cdot x_{ij}, \qquad i = 1 \ldots C, \quad j = 1 \ldots N. \tag{5.9}$$

Where the equilibrium ratio K_{ij} is computed from the relations that describe a vapour liquid equilibrium (VLE).

A vapour and liquid phase are in equilibrium, when the fugacities in the vapour f_i^V and liquid f_i^L phase for each species i are equal [2]

$$f_i^V = f_i^L, \qquad i = 1 \ldots C. \tag{5.10}$$

This can also be written in terms of the, liquid activity coefficient γ_i, the pointing factor F_{Pi}, the reference vapour fugacity coefficient φ_i, the vapour pressure p_i^S as well as the system pressure p along with the vapour and liquid molar fractions

$$\gamma_i \, F_{Pi} \, \varphi_i^0 \, p_i^S \, x_i = \varphi_i \, p \, y_i, \qquad i = 1 \ldots C. \tag{5.11}$$
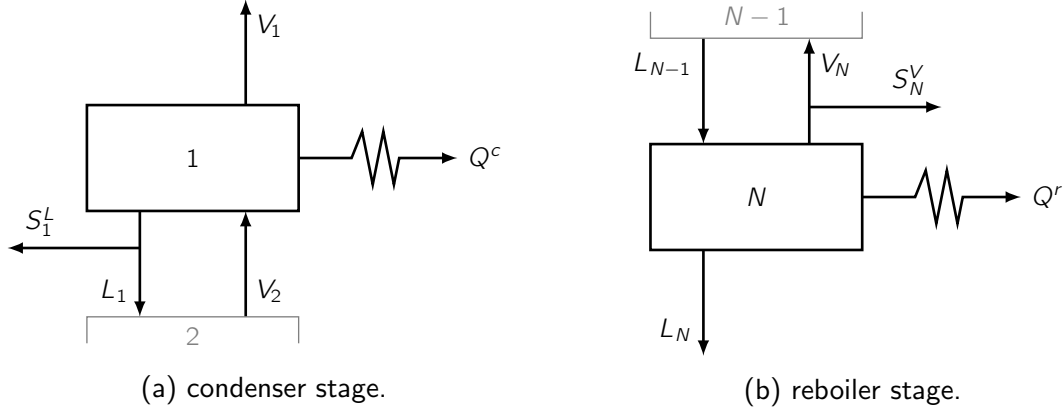
(a) condenser stage.

(b) reboiler stage.

By reformulating eq. (5.12) an expression for the equilibrium ratios can be derived

$$y_i = \underbrace{\frac{\gamma_i \, F_{Pi} \, \varphi_i^0 \, p_i^S}{\varphi_i \, p}}_{K_i} x_i, \qquad i = 1 \ldots C. \tag{5.12}$$

The equations to determine the quantities used when computing the equilibrium ratios are by themselves functions of temperature, pressure, and vapour as well as liquid molar fractions. They are further discussed in sec. 5.4. It therefore becomes evident that the equilibrium ratios are a major source non-linearities in the MESH equations.

Enthalpy balances The enthalpy balances can again be written using the previously defined stripping factors and splitting variables

$$0 = \left(1 + s_j^V\right) \cdot V_j \cdot h_j^V + \left(1 + s_j^L\right) \cdot L_j \cdot h_j^L - V_{j+1} \cdot h_{j+1}^V$$

$$- L_{j-1} \cdot h_{j-1}^L - \sum_{k=1}^{F^V} \zeta_{kj} \cdot F_k^V \cdot h_j^{FV} - \sum_{l=1}^{F^L} \zeta_{lj} \cdot F_j^L \cdot h_j^{FL} - \zeta_j^R \cdot V_N \cdot h_N^V,$$

$$i = 1 \ldots C, \quad j = 1 \ldots N, \quad k = 1 \ldots F^V, \quad l = 1 \ldots F^L. \tag{5.13}$$

Condenser and reboiler Condenser and reboiler are modeled more or less as regular column stages. However they possess certain specialties that are explicitly considered in the column model. For one it is assumed that no feeds enter the reboiler and condenser stage. Furthermore no vapour side stream is drawn from the condenser stage and no liquid side stream from the reboiler stage.

Additionally the condenser stage needs to examined a little further. In terms of operations several assumptions can be made for the condenser. In general one can distinguish a total, partial vapour and partial vapour liquid condenser. For the total condenser all vapour that enters the respective stage is condensed and only liquid product is drawn (here modeled as a side draw). The partial vapour condenser condenses only the vapour the is fed back into the column and all product that is drawn is gaseous. The partial vapour liquid condenser denotes the most general case, where part of

the incoming vapour is condensed and product ist drawn as vapour and liquid. The most important thing to consider in these different cases, is that while in both partial condensers a vapour liquid equilibrium takes place, due to the absence of vapour the same does not hold for the total condenser. To accommodate that fact the MESH equations have to be adjusted [16]. While the material and energy balances remain unchanged the equilibrium equations have to be altered. First the vapour and liquid compositions are set equal for all but one component

$$x_{i1} = y_{i1} \qquad i = 1 \dots C - 1, \tag{5.14}$$

and the condenser temperature is determined by the bubble point equation

$$0 = 1 - \sum_i K_{i1} \cdot x_{i1} \qquad i = 1 \dots C. \tag{5.15}$$

When implementing the model in a process simulator it is sensible to consider, that due to the limited accuracy of computers the omitted component in eq. (5.14) needs to a non-trace component in the condenser stage. The implemented model therefore as to specify such a component when a total condenser is chosen to avoid numerical difficulties.

In practice it is highly unlikely, that the exact amount of energy required to condensate all liquid will be drawn from the condenser. More likely, if all vapour is condensed, a little more energy will be withdrawn and slightly sub-cooled liquid will leave the condenser. Therefore the model includes the possibility to specify a degree of sub-cooling T^{sub} which will be considered when calculating the equilibrium ratios.

5.1.2 Specifications

The equation systems presented above is comprised of NC component balances, NC equilibrium equations, $2N$ summation equations and N energy balances. This gives a total of $N(2C + 3)$ equations. On the other hand there are N temperatures and pressures, $2N$ molar flow rates, N energy streams, and NC vapour as well as and liquid concentrations. Additionally the feed flow rates compositions and temperatures and the side draw split fractions or flow rates appear as variables. The feeds and side draws would usually be specified, which leaves a total of $N(2C + 5)$ variables.

The pressure profile of a distillation column is usually specified. Either by explicitly assigning a given pressure to each stage, or more conveniently by defining a pressure either the top or bottom pressure as well as the pressure drop per stage

$$\Delta p_{stage} = p_i - p_{i-1}, \qquad i = 2 \dots N. \tag{5.16}$$

In terms of unit operations this pressure drop is of high significance, as many columns can only be feasibly operated, if the pressure drop does not exceed certain limits. In case of the ASU the production of Argon only became feasible as structured packings, which display a very low pressure drop, became available. This is due to the large number of theoretical stages required to attain the desired Argon purities.

add pressure profile adjustment for optimization case – give reasons.

specification	replacement for H_1	replacement for H_N
reflux or boilup ratio	$0 = L_1 - \nu^D \cdot (V_1 + S_1^L)$	$0 = V_N - \nu^R \cdot L_N$
temperature	$0 = T_1 - T_{spec}$	$0 = T_N - T_{spec}$
product flowrate	$0 = (V_1 + S_1^L) - D$	$0 = L_N - B$
component product flowrate		$0 = L_N \cdot x_{iN} - b_i$
mole fraction	$0 = y_{i1} - y_{i,spec}$	$0 = x_{iN} - x_{ispec}$

Table 5.1: discrepancy functions for different column specifications.

The energies Q_i denote addition heaters or cooler on the respective stages. For all intermediate stages these values would be specified as well. If all energies would be specified, that would – along with the pressure profile – sum up to $2N$ specifications, which leaves $N(2C + 3)$ unknowns. As the number of equations and unknowns are the equal, this system can them be solved.

In practice it is often challenging to correctly guess the condenser and reboiler heat loads in advance. This is especially true since they have a tremendous impact on the overall performance of the column. Hence it is often desirable to supply other specifications than the respective heat loads. To allow for such specification so called discrepancy functions can be introduced [13], which replace the energy balance for the condenser and / or reboiler stage.

One common specification is the so called reflux ratio $\nu^D = \frac{L_1}{V_1 + S_1^L}$ for the condenser, or the boilup ratio $\nu^R = \frac{L_N}{V_N}$ for the reboiler. They are defined as the ratio of the molar flowrate sent back into the column over the product flowrate which leaves the column. For the reboiler this denotes a liquid stream, while for the condenser the product can be gaseous and liquid. Specifying this leads to

$$0 = L_1 - \nu^D \cdot (V_1 + S_1^L), \tag{5.17}$$

$$0 = V_N - \nu^R \cdot L_N, \tag{5.18}$$

as discrepancy functions. I addition to that further specifications are conceivable. Most commonly distillate (D) or bottoms (B) flow rates, or purities, component flow rates (d_i, b_i) or temperatures. The corresponding discrepancy functions are summarized in tab. 5.1.

The specifications for the reboiler stage are quite straightforward, in contrast to that, different cases for the condenser have to be considered. In the most general case the top product can be drawn as vapour and liquid. This case is here called a partial vapour liquid condenser. The other cases are a total condenser, where all the vapour entering the condenser stage is condensed, and all product is drawn as a liquid stream, as well as a partial vapour condenser, where only the reflux is condensed and all product is drawn as vapour. As discussed earlier no VLE takes place in the condenser stage, if a total condenser is specified, which needs to be accounted for. Both the total and partial vapour condensed implicitly include an extra specification since in former case the top vapour product flow rate becomes zero and in the latter the top liquid product flowrate. Furthermore a specification of the condenser energy is infeasible as well as implicitly given for the total condenser. In case of the partial vapour liquid condenser no implicit specification is given, which requires an additional specification. In general two top specifications are necessary, whereas only one bottom specification is required. These top specification can include the condenser duty, any top flowrate, the reflux ratio as well as a newly introduced quantity, the top vapour fraction defined as

$$\nu^{vap} = \frac{V_1}{V_1 + S_1^L}. \tag{5.19}$$

5.1.3 Column initialization

As mentioned before the solution of the MESH equations can pose a considerable problem to numerical solvers. It is therefore necessary to supply the solver with feasible estimates for the involved variables that can be used as an initial guess to facilitate convergence of the process model. A lot of effort has been spend to formulate robust strategies to initialize distillation column models. One of the most prominent is the so called Inside-Out algorithm first introduced by Boston and Sullivan [6]. Within this algorithm an inner and outer iterative loop are employed. Within the outer loop approximate parameters for simplified models of phase equilibrium and enthalpy are computed by rigorous thermodynamic models and guesses for stage temperatures and concentrations. Within the inner loop new stage temperatures and concentrations are by solving the MESH equations using the simplified thermodynamic models. Once the inner loop converges the simplified model parameters are updated within the outer loop by means of the newly calculated temperatures and concentrations. This algorithm converges in many cases even for very poor initial guesses and has been extended to handle complex columns with side-draws and even reactive distillation [7]. It is still in use in the process simulator Aspen Plus®. However as it is used within an modular algorithmic environment it is not applicable to equation based simulators such as gPROMS®.

More recently other approaches have been published to attain improved initial guesses. Fletcher and Morton [10] proposed the solution of a column model at infinite reflux and zero feed flow rate. This leads to a much simplified model which can be solved more easily. The computed purities and stage numbers can give valuable insight into the process model. As this approach relies on the solution of a simplified model and has no algorithmic elements, it can be implemented in equation based process simulators.

Another strategy that has been successfully applied to zeotropic and azeotropic mixtures relies on solving the column model for the limiting case of the adiabatic column [4]. The adiabatic column in this case is the column with the minimal entropy production in a real column. To avoid entropy production all streams that come in contact must be in equilibrium. To achieve this the column would have to employ an infinite number of stages and have an infinite number of heat exchangers along its length. The adiabatic column then uses only two heat exchanger in the condenser and reboiler stage and assumes a pinch point at the feed stage.

elaborate on adiabatic column

Furthermore a much simpler approach has proven adequate for many applications [13] which is also employed as a starting point in this work. There feed properties are used as initial guesses. First a linear temperature profile form the boiling temperature to dew temperature of the feed is used to initialize temperatures, whereas a simple flash at average column pressure and feed temperature yields a vapour and liquid concentration that which is used as uniform profile for every column stage. However as the feed might be sub-cooled liquid or super-heated vapour the TP-Flash is replaced by a specified vapour fraction. As vapour fraction for the flash initial estimates of the vapour and liquid flow rates at the top and bottom of the column are used. The stage-wise molar flow-rates are computed from the constant molal overflow assumption.

While this approach leads to model convergence in many cases, it is not entirely robust. While the system considered in this case displays only moderate non-idealities it is highly cupeled. Especially the low pressure column (LPC) has multiple feeds and side draws, which leads to non-convergence if the aforementioned initialization strategy is employed. However the fact that the system is not

highly non-ideal can be exploited. Whenever the K-values are not too much dependent on mixture composition an intermediate step can be used to refine concentration guesses. The constant molal overflow assumption is retained and the equilibrium ratios are computed based on the initial guesses from the first stage. The component balance is then reformulated only in terms of liquid component flow-rates l_{ij}

$$0 = \left((1 + s_j^V) \cdot K_{ij} \cdot \frac{V_j}{L_j} + (1 + s_j^L) \right) \cdot l_{ij} - \frac{V_{j+1}}{L_{j+1}} \cdot K_{ij+1} \cdot l_{ij+1} - l_{ij-1}$$
$$- F_j^V \cdot z_{i,j}^V - F_j^L \cdot z_{i,j}^L, \qquad i = 1 \ldots C, \quad j = 1 \ldots N. \quad (5.20)$$

eq. (5.20) is linear in the liquid component flow rates. Furthermore vapour component flow rates are substituted in the linear component balance and can be computed by

$$0 = v_{ij} - K_{ij} \cdot \frac{V_j}{L_j} \cdot l_{ij} \qquad i = 1 \ldots C, \quad j = 1 \ldots N. \qquad (5.21)$$

On of the reasons eq. (5.20) is formulated in terms of component flow rates rather than molar fractions, is that the molar fraction computed in that manner would not be normalized. If the mole fractions are computed from the component flow rates normalization is implicitly given

$$x_{ij} = \frac{l_{ij}}{\sum_k^C l_{kj}} \qquad i = 1 \ldots C, \quad j = 1 \ldots N. \qquad (5.22)$$

$$y_{ij} = \frac{v_{ij}}{\sum_k^C v_{kj}} \qquad i = 1 \ldots C, \quad j = 1 \ldots N. \qquad (5.23)$$

The total molar flow rates used in eq. (5.20) are computed by solving stage-wise total mass balances under the constant molal overflow assumption. This assumption postulates that the heat of vaporization is independent of system composition. Therefore always the same amount of liquid enters and leaves a given stage

$$0 = L_j + S_j^L - L_{j-1} - (1 + q_F^L) \cdot F_j^L - q_F^V \cdot F_j^V \qquad j = 1 \ldots N. \qquad (5.24)$$

Only at feed and side draw stages the total flow rates change. To introduce some more accuracy to the model, the available information about the feed is considered. When a feed enters as super-heated vapour or sub-cooled liquid, it has the capability to evaporate some liquid or liquefy some vapour. To account for that fact the feed energy parameters q_F^L and q_F^V are introduced

$$q_i^{FV} = \frac{H_i^{FV} - H_i^V}{H_i^V - H_i^L}, \qquad i = 1 \ldots F^V, \qquad (5.25)$$

$$q_i^{FL} = \frac{H_i^{FL} - H_i^L}{H_i^V - H_i^L}, \qquad i = 1 \ldots F^L. \qquad (5.26)$$

The vapour total flow rates are then computed from the total mass balances

$$0 = L_j + S_j^L + V_j + S_j^V - L_{j-1} - V_{j+1} - F_j^L - F_j^V, \qquad j = 1 \dots N. \tag{5.27}$$

As no energy balances are included at this stage, the condenser and reboiler stage are characterized by the reflux ($\nu^c = \frac{V_1}{L_1}$) or boilup ratio ($\nu^r = \frac{V_N}{L_N}$) respectively. This leads to

$$0 = V_1 - \nu^c \cdot L_1, \tag{5.28}$$
$$0 = L_N - \nu^r \cdot V_N. \tag{5.29}$$

To close the equation system the global mass balance is included

$$0 = V_1 + L_N + \sum_{j=1}^{N} (S_j^V + S_j^L - F_j^V - F_j^L), \qquad j = 1 \dots N. \tag{5.30}$$

Init specification

At this point it should be mentioned, that not all specifications are compatible with the initialization procedure. As no energy balances are solved during initialization, specified condenser or reboiler duties cannot be considered in this stage. Furthermore purity specifications are also not applicable during this stage, they are computed by a different approach. Due to that it is necessary – when duties or purities are specified – to supply substitute specifications, that can be used during initialization. Essentially all specifications concerning top and bottom flow rates and flow ratios are usable during initialization. The user interface implemented specifically asks for substitute specifications if any aforementioned cases are encountered.

Example

To illustrate how the initialization procedure works an example has been constructed of a rather complex column – or column section – with multiple feeds and side draws (fig. 5.2). It is taken from an example process of cryogenic air separation. The column in question is a column section without an condenser stage and displayed the most difficulties in terms of convergence when constructing the process flowsheet.

In addition to the aforemention initialization strategy, columns with side draws present are handled in a slightly different manner. Initially the side draws are disregarded. Then the initialization procedure is carried out. Once the column without side draws has converged, a homotopy approach

$$f(\mathbf{x}) = (1 - \alpha) \cdot f_0(\mathbf{x}) + \alpha \cdot f_1(\mathbf{x}) \tag{5.31}$$

is employed, where the parameter α is initially set to zero and then gradually moved to a value of one. During the initialization homotopies could generally be employed to move from one step to another. While in some cases robustness is improved by such a strategy, it is always computationally far more expensive then simply jumping between different stages.

For clarity reasons the different steps of the initializations procedure a repeated in a tabular manner

mention problems and bounded homotopy?

Figure 5.3: example column.
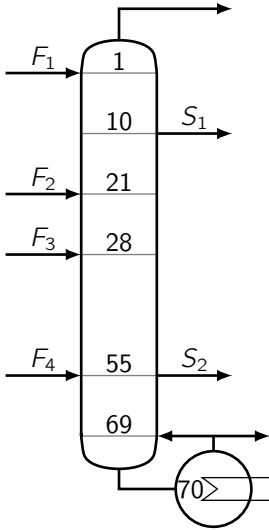
	feed specifications					
stream	flow $[\frac{kmol}{hr}]$	$z_{O_2}[-]$	$z_{N_2}[-]$	$z_{Ar}[-]$	$T[K]$	$p[bar]$
F_1	2985.77	4.674E-10	0.9999	6.378E-7	79.45	1.3
F_2	1836.36	0.2095	0.7812	0.0093	98.91	1.3
F_3	7609.06	0.2920	0.6950	0.0130	81.88	1.3
F_4	774.94	0.9161	5.393E-12	8.394E-2	92.13	1.8

	column specifications				
stages	S_1 frac	S_2 frac	boilup ratio	p^{top}	p^{bot}
70	10	0.15	3.5	1.2 bar	1.3 bar

Table 5.2: column specifications.

1. • linear temperature profile between dew (T^{dew}) and bubble point temperature (T^{bub}) of mixed feed.
   • linear profile between feed flash vapour and liquid compositions for liquid stage compositions.
   • constant profile for vapour compositions.
   • molar flow rates from constant molar overflow model.
   • side draw flow rates set to zero.

2. • total molar flow rates form constant molar overflow model.
   • simplified equilibrium ratios from initial liquid mole fractions and linear temperature profile.
   • liquid and vapour mole fractions from linearized mass balances.

3. rigorous solution of MESH equations with side draws still set to zero.

4. homotopic approach to MESH equations with side draws considered.

The resulting profiles for oxygen and nitrogen concentrations in the example column can be seen in fig. 5.4a and fig. 5.4b.

5.2 Compression & liquefaction

The issue of cooling the ambient air to process temperatures at around 90 K is not an easy one. The main hindrance is, that a heat sink at this temperature level is not readily available. Lucky thermodynamics offer a different way to reach such temperatures. In order to do so, the ambient air first needs to be compressed and then expanded again. Cooling then occurs by either exploiting the *Joule-Thompson* effect or isentropic expansion. First a few comments are made about the compression stage, while afterwards the governing principles for cooling by expansion will be described.
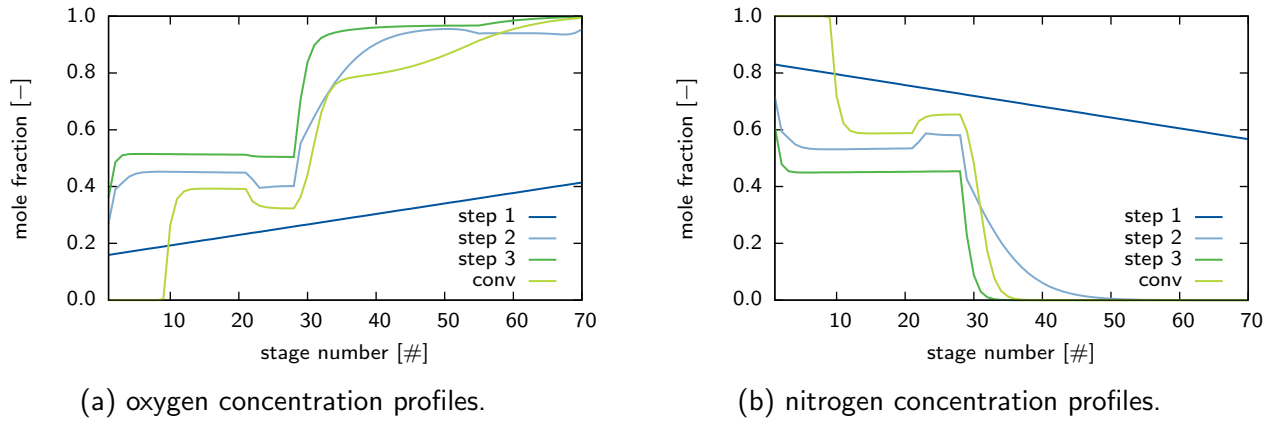
(a) oxygen concentration profiles.

(b) nitrogen concentration profiles.

Figure 5.4: initialization example concentration profiles.
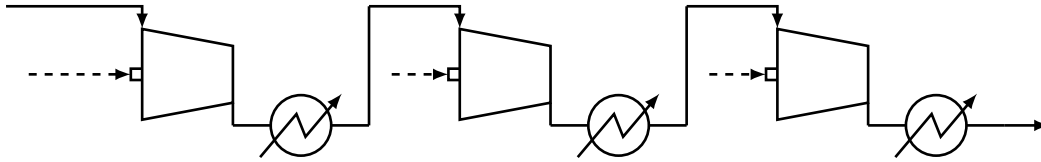
Multi-stage compression

Figure 5.5: Multi-stage compression.

Compressors and expanders are among the most common process equipment. A multitude of processes utilizes them as primary or auxiliary units. While the tasks performed by especially the compressors is essential for reaching the required process temperatures, they have less impact in terms of process performance and capital expenditure.

The rigorous modeling of continuous flow machines in terms of unit operations poses great challenges. For specific units it may be undertaken by means of CFD simulations or employing characteristics diagrams, which require extensive experiments and can usually be obtained from the manufacturer. For the purposes of process design however a simpler approach with unit efficiencies is appropriate.

In order to attain the desired compression it is beneficial, to use a multi stage compressor with inter-cooling as depicted in fig. 5.5. This yields a lower energy consumption as a single stage unit for the same compression ratio.

Cooling by expansion

The liquefaction of gases requires temperatures well below ambient conditions. In order to reach such conditions one cannot utilize natural occurring coolants, but rather cooling effects that occur during the expansion of compressed gases. First we consider the expansion through an expansion valve or so called *Joule-Thompson* - valve. If we assume very good insulation of conditions this expansion can closely be approximated by an isenthalpic process ($h_1 = h_2$). To describe the change in temperature
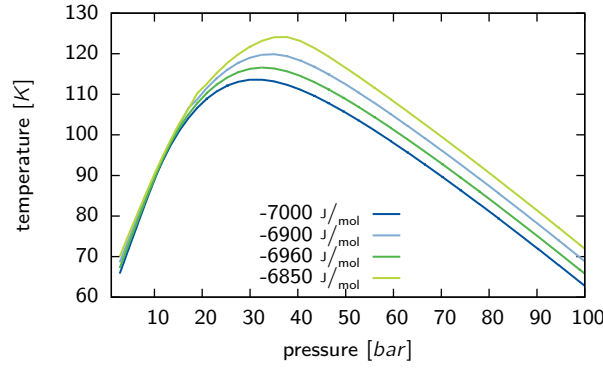
31

Figure 5.6: Isenthalpes computed by Peng-Robinson model.

during isenthalpic expansion the *Joule-Thompson* coefficient

$$\mu_{JT} = \left(\frac{\partial T}{\partial p}\right)_h ,$$ (5.32)

which denotes pressure derivative of the temperature at constant enthalpy can be considered. This can be transformed into

$$\mu_{JT} = \frac{1}{c_p}\left[T\left(\frac{\partial v}{\partial T}\right)_p - v\right]$$ (5.33)

If we employ the Peng-Robinson equation of state we can plot the isenthalpes for ambient air ($x_{N_2} = 0.7812$, $x_{O_2} = 0.2095$, $x_{Ar} = 0.0093$) in a PT-diagramm (fig. 5.6). One can easily see, that in certain ranges a pressure decrease will result in an increase in temperature, while for other regions in a decrease. It is interesting to mention that the non-idealities of a given gas give rise to this effect. For an ideal gas the temperature change at isenthalpic expansion would always be zero. Luckily for the cryogenic engineer real gases deviate from ideal behaviour especially at elevated pressures and low temperatures. It is therefore important to give some consideration to the thermodynamic model used to describe the properties of the system in question, as the non-ideal properties need to be captured appropriately.

A different way of expanding a compressed gas, is by letting it produce work in an fluid kinetic machine. If one assumes an adiabatic devices and disregards irreversible effects, this process can be viewed as isentropic. Analogous to the isenthalpic case an isentropic expansion coefficient can be defined

$$\mu_S = \left(\frac{\partial T}{\partial p}\right)_S = \frac{T}{c_p}\left(\frac{\partial v}{\partial T}\right)_p .$$ (5.34)

Here the derivative in the second form corresponds to the volumetric coefficient of thermal expansion β, which is always positive for gases, which in turn means, that an isentropic expansion will always result in an temperature decrease, whereas the isentropic expansion only led to a decrease in certain

elaborat on different terms.

add derivative in appendix?

cases. Furthermore an isentropic expansion over the same pressure range will always result in lower temperatures than an isenthalpic expansion. Additionally work can be recovered. The reason that isentropic valves are most commonly used in liquefaction systems, is that those work producing machines cannot handle significant phase changes, which is after all the desired result of liquefaction.

Traditionally only the isenthalpic expansion had been used within the cryogenic air separation process, since – as mentioned before – the air needs to be liquefied in order to be fed into be distilled. However in modern process configurations the isentropic expansion is also considered, and partial streams are fed into the low pressure column in gaseous form.

5.3 Heat exchange

The issue of heat integration is essential to the economic performance of cryogenic air separation. Foremost one must consider the special column configuration used in the process. Since operation of the condenser in the low pressure section only becomes possible if the reboiler in the high pressure section functions as heat sink, no external utilities are supplied to either unit. Rather they are combined into a single heat exchange unit. Thus the absolute value of the reboiler energy must be equal to the energy recovered from the condenser. Furthermore the material streams entering the process can – and should – exchange heat with the process streams leaving it. The combined condenser / reboiler for LPC / HPC column is assumed as a given heat exchange. This males sense insofar, as this is a necessity in terms of the actual physical implementation of the process units. Also the usage of the oxygen rich liquid from the HPC as coolant in the Argon condenser is assumed as fixed.

This leaves the process stream leaving the compression stage of the process as well as all product and waste streams leaving the process. All those streams are – for simulation purposes – fed into a single multi-stream heat exchange unit. To model this unit a simple model is employed which essentially consists of one single enthalpy balance

$$0 = \sum_i H_i^{out} - H_i^{in}, \qquad . \tag{5.35}$$

The enthalpy streams H_i^{in} and H_i^{out} are determined by their respective material stream, their compositions, pressures and temperatures. All inlet values are supplied by the surrounding process flowsheet. The outlet material streams are equal to the inlet values, as no reactions or material exchange takes place within the unit. The outlet pressure is determined by a specified pressure drop over the unit. This pressure drop might be specified for each stream separately but in this context a single value seems more reasonable. This leaves the outlet temperatures as free variables. However as we are dealing with one single equation, consequently the degree of freedom for this model is one, meaning all but one one outlet temperature have to be supplied.

Apparently this approach exhibits several shortcomings. For one the need to specify all but one temperature is unsatisfactory. In addition to that none of the principles of heat integration are considered in this model. Neither are there facilities to check whether any energy would be transported across a pinch point, nor is it assured, that the minimum driving force criteria is not violated. Even more essential, no pairing of hot and cold streams that would exchange heat is undertaken. All

those aspects are usually examined separately by means of an composite curve or other tools for heat integration. Recently an alternative approach for simultaneous heat integration and process optimization has been proposed [14]. The approach presented there is also able of handling phase changes. However it is associated with considerable computational effort. As the ASU process, is quite expensive as it is it was decided to exclude this approach for the time being and manually check the thermodynamic feasibility of converged solutions.

5.4 Thermodynamic models

Aside from the unit operation models, the behaviour of materials in a process needs to be adequately accounted for. This is done by means of so called equations of state (EOS) and excess Gibbs energy models. In terms of thermodynamics there are only a limited amount of variables. Namely the pressure, density and temperature as well as composition. While equations of state can model a given system in the vapour as well as liquid phase, excess Gibbs energy models only account for the behaviour of a liquid and need to be used in conjunction with other models for the vapour phase. However they have shown considerable better performance for highly non-ideal systems [2]. As mentioned earlier (sec. 5.2) it is essential to accurately capture the non-idealities of air in order to capture the liquefaction process. In the case of cryogenic air separation, the Peng-Robinson as well as the Benders equation of state have shown satisfactory performance. The Peng-Robinson equation was chosen to be used in the presented model

$$p = \frac{RT}{V - b} - \frac{a_c \left[1 + m \left(1 - \sqrt{T_r}\right)\right]^2}{V^2 + 2bV - b^2} \tag{5.36}$$

$$m = 0.37464 + 1.54226\omega - 0.26992\omega^2 \tag{5.37}$$

$$a_c = 0.45724\frac{R^2 T_c^2}{p_c} \tag{5.38}$$

$$b = 0.077796\frac{RT_c}{p_c} \tag{5.39}$$

$$\omega = -1 - \log_{10} \left(p_r^{sat}\right)_{T_r=0.7} \tag{5.40}$$

However the Peng-Robinson EOS relies on the so called one-fluid theory which models each fluid as pure. To model mixtures the pure component parameters have to be "mixed"

$$a = \sum_{i=1}^{C} \sum_{j=1}^{C} y_i y_j a_{ij}, \tag{5.41}$$

$$a_{ij} = \sqrt{a_i a_j}(1 - k_{ij}), \tag{5.42}$$

$$b = \sum_{i=1}^{C} y_i b_i. \tag{5.43}$$

From that EOS numerous relevant properties such as excess enthalpy, fugacity coefficients or densities can be calculated. For a list of some relevant equations refer to sec. A.1.

which properties should be included? Or

5.5 Economic models

As discussed earlier economic consideration play a major role in process design. In order to account for the process economics the cost of the process to be implemented needs to be estimated at the design level. However as limited information is available estimation methods have to be employed. In sec. 4 the general approach for cost estimation of process equipment was introduced, where a specific value such as heat-exchange area or vessel size is used to approximate equipment cost. However for more specific units extended models are available, where statistical data is employed to yield a more realistic fit to cost data. The cost functions and correction factors presented in this chapter are, if not stated otherwise, taken from [19]. Also unless otherwise stated the unit cost is given for the year 2006 ($CE = 500$).

Destillation column

Out of all the process equipment the distillation column probably is the most elaborate unit. It also poses the greatest challenges when it comes to finding an appropriate estimate for its cost. This is die to the fact that the column in itself is rather large and complex. To properly operate a column the vessel needs to have numerous valves, scaffolding and several manholes. Due to its size further factors come into play that need not to be considered for the other relatively small units. Those location dependent factors might include resilience towards earthquakes, the ability to withstand close winds or intensive ambient temperatures. However as the scope of this work explicitly focuses on early design stages those location specific influences will be disregarded to arrive at simpler models for cost estimation.

Vertical tower The cost for the vessel C_V which is to be vertically erected vertically is dependent on teh weight fo the weight W ($[lbs]$) of the vessel. This includes valves, manholes and other details directly connected with the tower. However the cost for ladders, platforms and railings necessary to properly operate the column are calculated separately

$$C_p = f_M \, C_V + C_{PL}.\tag{5.44}$$

The correlated equation for the cost of the tower is given by

$$C_V = \exp\left\{7.2756 + 0.18255 \cdot \ln[W] + 0.02297 \cdot (\ln[W])^2\right\}, \qquad 9000 \leq W \leq 2.5 \cdot 10^6.\tag{5.45}$$

To the cost of the tower, the cost of the surrounding support structure ist added. It is dependent on the inner diameter of the vessel (D_i) as well as the so called tangent to tangent length (L). This denotes the length of the tube that makes up the vessel excluding the spherical domes that close the column on each side. With that the additional cost is then computed by

$$C_{PL} = 300.9 \cdot (D_i)^{0.63316} \cdot (L)^{0.80161}.\tag{5.46}$$

Weight As can be seen from the above correlations the weight of the column is a determining factor for the estimated and actual cost. Therefore some thought should be put into how this can be determined, when the final design is unknown. Again several correlations have been applied to real life units which yield satisfactory results. In general the weight of the empty vessel can be computed by determining the volume of the material and multiplying it with its density (ϱ)

$$W = \pi(D_i + t_s)(L + 0.8 \cdot D_i)t_s \cdot \varrho. \tag{5.47}$$

The term $0.8D_i$ is included to approximate the weight of the domes, whereas t_s is the shell thickness. To determine how thick the walls of the shell need to be the ASME pressure vessel code formula is often applied

$$t_s = \frac{P_d\, D_i}{2\, S\, E - 1.2 P_d}. \tag{5.48}$$

Where the maximal allowable stress S, which the chosen material can withstand at process conditions is multiplied by the fractional weld efficiency E to regard the effects of the manufacturing process on the material strength. To ensure an error on the side of caution the design pressure P_d is calculated from the actual operating pressure P_o by means of

$$P_d = \exp\left\{0.60600 + 0.91615 \cdot (\ln[P_o]) + 0.0015655 \cdot (\ln[P_o])^2\right. \tag{5.49}$$

It is important to consider, that the maximum allowable stress especially needs to take into account the operating temperature of the distillation process, as it might have significant effects.

Furthermore the given formulas only apply to pressures above ambient conditions. Thus low pressure or vacuum distillation is not covered by the presented formulas.

Column internals While internal support structures are already considered by the equations given above, the internals responsible to ensure product separation are not. Those make up a very significant amount of the total column cost and are available .

finish column internals

Centrifugal pump

Pumps are among the most common units of process equipment. While there are several different kinds of pumps that can be used, the centrifugal pump is one of the most popular choices and denotes a very likely choice for the process conditions considered in this application. Hence other pump types will not be considered at this point.

Pump In terms of operations pumps are best described by the volumetric flow transported Q as well as the pump head H, the hight that needs to be overcome. Data taken from the company Mosanto was used to correlate the pump cost to a specific value

$$S = Q\sqrt{H}. \tag{5.50}$$

number of stages	shaft rpm	case-split orientation	flow rate range ([gpm])	pump head range ([ft])	maximum power ([Hp])	type factor f_T
1	3600	VSC	50 - 900	50 - 400	75	1.00
1	1800	VSC	50 - 3500	50 - 200	200	1.50
1	3600	HSC	100 - 1500	100 - 450	150	1.70
1	1800	HSC	250 - 5000	50 - 500	250	2.00
2	3600	HSC	50 - 1100	300 - 1100	250	2.70
2+	3600	HSC	100 - 1500	650 - 3200	1450	8.90

Table 5.3: Pump type factors [19].

material of construction	material factor
cast iron	1.00
ductile iron	1.15
cast steel	1.35
bronze	1.90
stainless teel	2.00
Hastelloy C	2.95
monel	3.30
nickel	3.50
titanium	9.70

Table 5.4: Pump material factors [19].

As a reference unit the base price C_B is estimated for a cast iron single-stage vertically split case at 3600 *rpm*

$$C_B = \exp\left\{9.7171 - 0.6019 \cdot \ln[S] + 0.0519(\ln[S])^2\right\}, \qquad 400 \leq S \leq 100000. \qquad (5.51)$$

The most influential addition factors for the pump price are the material, which is accounted for in the material factor f_m, as well as the rotation, case split orientation (horizontal and vertical), the number of stages, covered flow rate range, pump head range and maximum motor power, which are all agglomerated in the type factor f_T. Values for these factors are given in tab. 5.3 and tab. 5.4.

Electric motor   Separately from the pump itself the motor to drive the compression is considered. While the volumetric flow and the pump head certainly are valid choices to correlate motors for pumps especially, the power consumption is a more general specific value

$$P_C = \frac{P_T}{\eta_P \eta_M} = \frac{P_B}{\eta_M} \qquad (5.52)$$

It can be calculated from the theoretic power of the pump P_T and the efficiencies η_P η_M. While an estimate for the expected power consumption might be already available at rather early design stages, the efficiencies will have to be correlated as well if resorting to average values is considered too coarse. Those correlations rely on the volumetric flow in gallons per minute ([gpm]) and the brake horse power $P_B = \frac{P_T}{\eta_P}$.

$$\eta_P = -0.316 + 0.24015 \cdot \ln[Q] - 0.01199 \cdot (\ln[Q])^2 \qquad 50 \leq Q \leq 5000 \qquad (5.53)$$

type motor enclosure	3600 rpm	1800 rpm
open, drip-proof enclosure, 1 to 700 Hp	1.0	0.9
totally enclosed, fan-cooled, 1 to 250 Hp	1.4	1.3
explosion-proof encosure, 1 to 250 Hp	1.8	1.7

Table 5.5: Type factors for different motor types.

$$\eta_M = 0.80 + 0.0319 \cdot \ln[P_B] - 0.00182 \cdot (\ln[P_B])^2 \qquad 1 \le P_B \le 1500 \tag{5.54}$$

After having calculated the power which the motor needs to supply its base cost of an open, drip-proof enclosed motor at 3600 rpm can be approximated by

$$C_B = \exp\left\{5.8259 + 0.13141 \cdot \ln[P_C] + 0.053255 \cdot (\ln[P_C])^2 \right.$$
$$\left. + 0.028628 \cdot (\ln[P_C])^3 - 0.0035549 \cdot (\ln[P_C])^4\right\} \qquad 1 \le P_C \le 700 \tag{5.55}$$

To adjust the cost for different types of electric motors the type factors from tab. 5.5

Compressor

The cost of compressors is correlated with their respective power consumption measured in horsepower. Although not the most efficient type of compressor, centrifugal compressors are very popular in the process industry, as they are easily controlled an deliver a very steady flow. However as different types might be employed as well base cost correlations for centrifugal, reciprocation and screw compressors are given.

Centrifugal compressor

$$C_B = \exp\left\{7.5800 + 0.80 \cdot (\ln[P_C])\right\} \qquad 200 \le P_C \le 30000 \tag{5.56}$$

Reciprocating compressor

$$C_B = \exp\left\{7.9661 + 0.80 \cdot (\ln[P_C])\right\} \qquad 200 \le P_C \le 20000 \tag{5.57}$$

Screw compressor

$$C_B = \exp\left\{8.1238 + 0.7243 \cdot (\ln[P_C])\right\} \qquad 200 \le P_C \le 750 \tag{5.58}$$

Again as with most other equipment types correction factors are used to adjust for different realization of this piece of equipment. Here type of motor as well as the construction material have the biggest effects on the unit price and are explicitly considered.

$$C_p = f_D \, f_M \, C_B \tag{5.59}$$

The alternatives to the electric motor ($f_D = 1.0$) are a steam turbine ($f_D = 1.15$) or a gas turbine ($f_D = 1.25$). It should however be noted that aside from being the cheapest choice, the electric motor is also the most efficient. Thus the turbines are mostly considered, when process steam or combustion gas is easily available, such that the drawbacks might be eliminated by not having to supply the electric energy for the electric motor. In terms of construction material all base costs are for cast iron or carbon steel. Some appliances may require more resistant and also more expensive materials such as stainless steel ($f_M = 2.5$) or an nickel alloy ($f_M = 5.0$).

Reboiler / condenser

Reboiler and condenser can be characterized as heat exchangers, and be handled in the same way, as the main difference is weather heat is transferred to or from the process stream. In that sense they must be distinguished when considering the operating cost, as the cost for hot or cold auxiliary streams might differ significantly. As customary for heat exchangers the specific quantity for cost correlations is the necessary heat exchange area A measured in ft.

Again the construction material as well as the operating conditions have an effect on the final cost

$$C_p = f_P \, f_M \, C_B. \tag{5.60}$$

The correction for pressures f_P takes into account the operating pressure P_o and is computed by

$$f_P = 0.8510 + 0.1292 P_o + 0.0198 * P_o^2. \tag{5.61}$$

The material correction factor f_M

$$f_M = \tag{5.62}$$

Shell and tube heat exchanger

$$C_B = \exp\left\{11.667 - 0.8709 \cdot (\ln[A]) + 0.09005 \cdot (\ln[A])^2\right\} \tag{5.63}$$

Double pipe

$$C_B = \exp\left\{7.146 + 0.1600 \cdot (\ln[A])\right\} \tag{5.64}$$

5.6 Cryogenic air separation process

The roots of cryogenic air separation lie in the first experiment and apparatus by Carl von Linde – founder of the Linde AG – which led to the first air separation plant in 1902. This earliest version of the an air separation plant consisted of a single column or one might argue even only half a column as it only possess a reboiler and no condenser). In 1910 the foundation of to the modern air separation
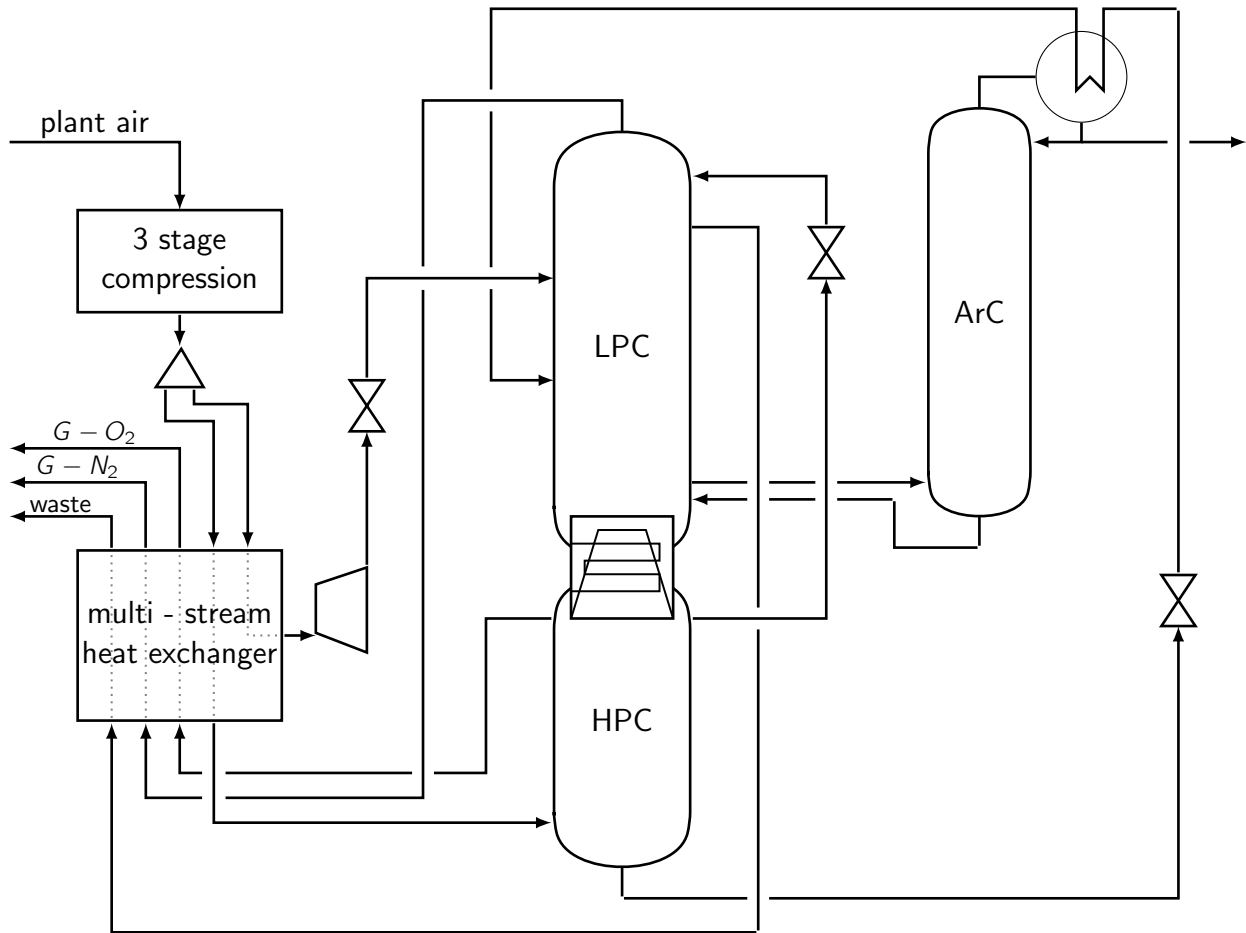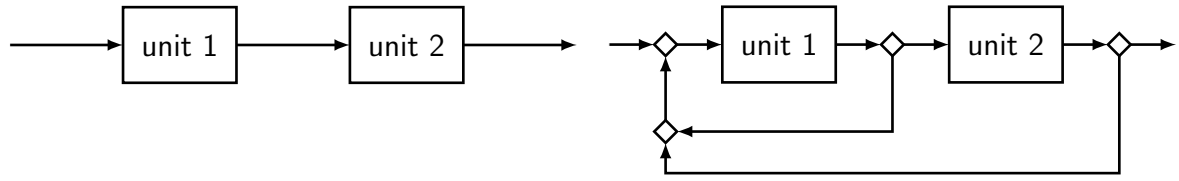
Figure 5.7: simplified cryogenic air separation process.

was set with the development of a double column plant. There each column operated at different pressures, which enabled the condenser and reboiler to be combined into a single heat exchange unit. This basic principle is in use to this day. However several enhancements have been made to to the original process design. Some were driven by new technological developments. Among the most prominent is the recovery of pure Argon – only a trace element in ambient air – within the process. Initially the Argon recovery had to be undertaken through the help of a catalytic converter. With the development of structured packings which display a very low pressure drop and height equivalent to theoretical stage (HEPT) it became feasible to separate Argon within a separate distillation column, as it requires a lot of theoretical stages, which would have previously led to infeasible large towers. Further advancements include internal compression which allows for compression of liquefied products within the cold box and more advanced designs of the condenser / reboiler unit.

For the purposes of this project a simplified version of an ASU has been considered. A process flowsheet is depicted in fig. 5.7.

5.6.1 Flowsheet initialization

Even for single unit models initialization might pose difficulties, when a whole process model is considered, this task might become even more difficult. If the process units are mainly sequential, the

(a) Feed forward process. (b) process with feedbacks.
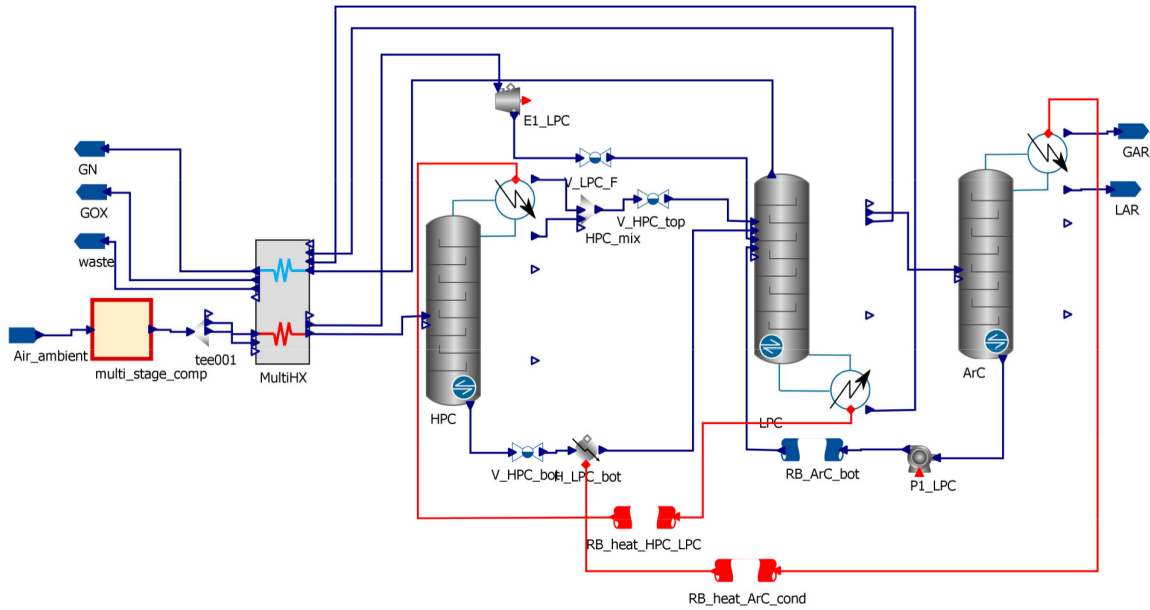
Figure 5.8: Different process configurations.

Figure 5.9: Implementation of simplified cryogenic air separation process in gPROMS.

task of initializing becomes no more difficult, then initializing the single units. But in most chemical processes a purely sequential arrangement of process equipment is not given. As soon as feedbacks are introduced into the process, the question of initialization becomes considerably more complex. In the most general case it is not even ensured, that a steady state of process operations even exists. As feedbacks are introduced, the process might become unstable or display oscillatory behaviour. Fig. 5.8a shows the concept for a purely feed forward process, while fig. 5.8b is an example for a process with feedbacks, in particular an arrangement with an inner and outer feedback loop.

As mentioned before feedbacks greatly complicate calculations for a given process. With the cryogenic air separation process this is especially true, since it is highly integrated and coupled. The only external cooling that is available comes from the initial compression and expansion of the ambient air. During the compression, since temperatures are still around ambient conditions and conventional coolants can be employed as heat sink. This is done during the multi-stage compression. All other heat exchange within the process can only be done against other internal process streams, as the process operates at conditions far away form ambient conditions. Far more than the feedbacks associated with material streams, it is the energy coupling that makes simulation of this process a non-trivial task. Especially, as the energies in condenser and reboiler of distillation columns have great effects on all operating condition.

Fig. 5.9 shows the flowsheet of the simplified ASU process depicted in fig. 5.7. In order the symbols in the material streams (blue) and energy streams (red) represend so called recycle breakers, which play a vital role during initialization of the flowsheet. The recycle breakers play no part in the converged flowsheet. Their function is to break the recycle or feedback loops in the process and transform the process into a feed forward process during initial computations. To achieve that, the recycle breakers are supplied with initial guesses for for all properties associated with the respective material or energy streams. For the energy recycle breakers the transformation from open to closed operation mode is rather simple. The outlet energy stream is merely moved from initial guess to inlet stream by means of eq. (5.31). For the material breaker one hast to invest a little more effort, as not all properties can be moved so easily while maintaining physical sense. The material stream and pressure are treated identically, while the temperature needs to computed from an enthalpy balance.

As for the concrete initialization procedure: first all recycle breakers are open and have the initial guesses at their outlet ports. Then all single units are converged. While this is done simultaneously in terms of the solution algorithm, the downstream units remain in the simplified stages of the unit respective initialization procedures wile the upstream units are solved with the rigorous models. Once all units have been converged, the recycle breakers are closed one after another. First the material stream between the Argon column (ArC) and the low pressure column (LPC), then the energy couple between the Argon condenser and and the oxygen rich material stream is closed. Finally the – maybe most important – connection between the LPC reboiler and HPC condenser is established.

6 Dynamic model

explain model development and the resulting equal number of liquid and vapour feeds...

6.0.2 MESH equations

**balance equations**

Total mass balance

$$\frac{\mathrm{d}n_j}{\mathrm{d}t} = V_{j+1} + L_{j-1} + \sum_{k=1}^{n_F} \zeta_{kj} \cdot F_j^V + \sum_{l=1}^{n_F} \zeta_{lj} \cdot F_j^L + \zeta_j^R \cdot V_N - \left(1 + s_j^V\right) \cdot V_j$$
$$- \left(1 + s_j^L\right) \cdot L_j \qquad i = 1 \ldots n_C - 1, \quad j = 1 \ldots N, \quad k = 1 \ldots F^V, \quad l = 1 \ldots F^L. \tag{6.1}$$

$n_C - 1$ component balances

$$\frac{\mathrm{d}n_{ij}}{\mathrm{d}t} = \left(1 + s_j^V\right) \cdot V_j \cdot y_{i,j} + \left(1 + s_j^L\right) \cdot L_j \cdot x_{i,j} - V_{j+1} \cdot y_{i,j+1}$$
$$- L_{j-1} \cdot x_{i,j-1} - \sum_{k=1}^{F^V} \zeta_{kj} \cdot F_j^V \cdot z_{i,j}^V - \sum_{l=1}^{F^L} \zeta_{lj} \cdot F_j^L \cdot z_{i,j}^L - \zeta_j^R \cdot V_N \cdot y_{iN},$$
$$i = 1 \ldots n_C - 1, \quad j = 1 \ldots N, \quad k = 1 \ldots n_F, \quad l = 1 \ldots n_F. \tag{6.2}$$

Total internal energy balance

$$\frac{\mathrm{d}U_j}{\mathrm{d}t} = \left(1 + s_j^V\right) \cdot V_j \cdot h_j^V + \left(1 + s_j^L\right) \cdot L_j \cdot h_j^L - V_{j+1} \cdot h_{j+1}^V$$
$$- L_{j-1} \cdot h_{j-1}^L - \sum_{k=1}^{F^V} \zeta_{kj} \cdot F_k^V \cdot h_j^{FV} - \sum_{l=1}^{F^L} \zeta_{lj} \cdot F_j^L \cdot h_j^{FL} - \zeta_j^R \cdot V_N \cdot h_N^V,$$
$$i = 1 \ldots n_C, \quad j = 1 \ldots N, \quad k = 1 \ldots n_F, \quad l = 1 \ldots n_F. \tag{6.3}$$
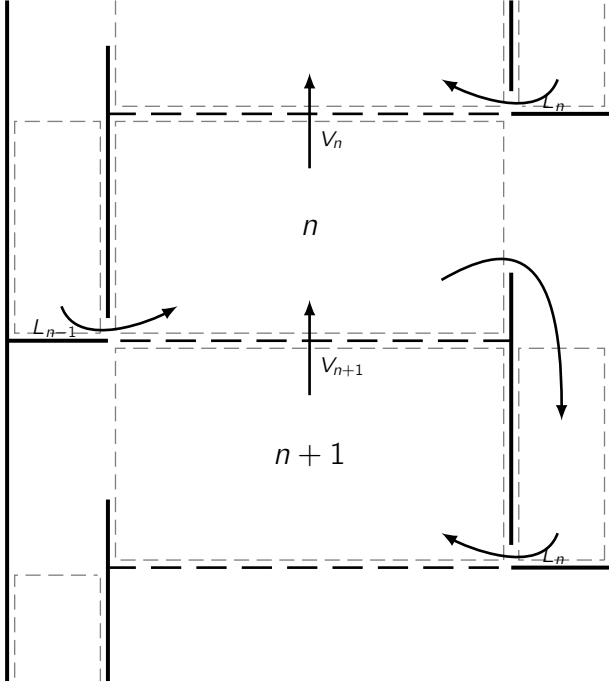
constituent equations

Equilibrium equations

$$y_{ij} = K_{ij} \cdot x_{ij}, \qquad i = 1 \ldots n_C \quad j = 1 \ldots N, \tag{6.4}$$

summation equations

$$1 = \sum_{i}^{n_c} y_{ij} \qquad j = 1 \ldots N, \tag{6.5}$$

$$1 = \sum_{i}^{n_c} x_{ij} \qquad j = 1 \ldots N, \tag{6.6}$$

holdup calculations

$$n_{ij} = x_{ij} n_j^L + y_{ij} n_j^V \qquad i = 1 \ldots n_C \quad j = 1 \ldots N, \tag{6.7}$$

$$U_j = n_j^L h_j^L + n_j^V h_j^V - p_j V_j \qquad j = 1 \ldots N, \tag{6.8}$$

$$V_j = V_j^L + V_j^V \qquad j = 1 \ldots N, \tag{6.9}$$

$$V_j^L = \frac{n_j^L}{\varrho_j^L} \qquad j = 1 \ldots N, \tag{6.10}$$

$$V_j^V = \frac{n_j^V}{\varrho_j^V} \qquad j = 1 \ldots N, \tag{6.11}$$

$$n_j = n_j^L + n_j^V. \tag{6.12}$$

hydraulic equations

$$h_{ow} = 0.68175 F_w \left(\frac{q_j^L}{h_w} \right)^{\frac{2}{3}} \tag{6.13}$$

$$n_j^L = \varrho_j^L A_j (h_w + h_{ow}) \tag{6.14}$$

$$L_j = \varrho_j^L q_j^L \tag{6.15}$$

$$p_j - p_{j+1} = (h_w + h_{j,ow}) \varrho_j^L g + 0.5 \xi \varrho_{j+1}^V \left(\frac{q_{j+1}^V}{A_h} \right)^2 \tag{6.16}$$

6.1 Models for columns with structured packings

- sections treated as trays
    - rate based models
        * film theory based models
    - equilibrium stage models
        * HETS / plate efficiency
- column divided into small (almost differential ?) sections
    - rate based models only

6.1.1 holdup & pressure drop

Model by Rocha et al.

equation for dimensionless holdup

$$h_t = \left(\frac{4 F_t}{S} \right)^{\frac{2}{3}} \sqrt[3]{\frac{3 \mu_L v_{LS}}{\varrho_L \sin(\theta) \varepsilon g_{eff}}} \tag{6.17}$$

correction factor for liquid holdup calculated ba Shi/Mersmann equation

$$F_{t,S-M} = \frac{29.12 \left(We_L \, Fr_L \right)^{0.15} S^{0.359}}{Re_L^{0.2} \varepsilon^{0.6} (1 - 0.93 \cos \gamma)(\sin \theta)^{0.3}} \tag{6.18}$$

$$g_{eff} = g \left(\frac{\varrho_L - \varrho_g}{\varrho_L} \right) \left[1 - \left(\frac{\Delta p / \Delta Z}{(\Delta p / \Delta Z)_{flood}} \right) \right] \tag{6.19}$$

$$\cos \gamma = \begin{cases} 0.9 & \text{if} \quad \sigma \le 0.055 \frac{N}{m} \\ 5.211 \cdot 10^{-16.835\sigma} & \text{if} \quad \sigma > 0.055 \frac{N}{m} \end{cases} \tag{6.20}$$

$$Re_L = \frac{\varrho_L v_L D}{\mu_L} \tag{6.21}$$

$$We_L = \frac{\varrho_L v_L^2 D}{\sigma} \tag{6.22}$$

$$Fr_L = \tag{6.23}$$

dry pressure drop with correlated friction factor funktion...

$$\frac{\Delta p_{dry}}{\Delta Z} = \underbrace{\frac{0.177\varrho_g}{S\varepsilon^2(\sin\theta)^2}}_{A} \cdot v_{gS}^2 + \underbrace{\frac{88.774\mu_g}{S^2\varrho\sin\theta}}_{B} \cdot v_{gS} = A v_{gS}^2 + B v_{gS} \tag{6.24}$$

Delft model

- valid in pre-load region
- adjustment by loading factor (Olujic 1999)

SPR method

- valid in pre-load region
- adjustment by loading factor (Olujic 1999)

Hydrodynamic analogy

- employ rigorous methods to solve hydrodynamics by superimposing solutions of easier scenarios

gas flow

- assume round channels with hydraulic diameter
- laminar fully developed flow
- ideal mixing at regular intervals to account for abrupt changes in gas flow directions at intersections

liquid flow

- continous thin film flow
- flow direction according to gravity flow angle
- laminar fully developed flow
- neglect of radial maldistribution
- ideal mixing at periodic intervals

equations   hydraulic diameter

$$d_h = \frac{b_0 h}{s_0} \tag{6.25}$$

gravity flow angle

$$alpha = \arctan \left(\frac{\cot \varphi}{\sin \left[\arctan \left(\cos \varphi \cot \frac{\gamma}{2} \right) \right]} \right) \tag{6.26}$$

undisturbed liquid flow

$$z_L = \frac{b_0}{2 \sin \left(\frac{\gamma}{2} \right) \sin \beta} \tag{6.27}$$

$$\beta = \arcsin \left(\sin \varphi \cos \epsilon \right) \tag{6.28}$$

$$\epsilon = \arctan \left(\cos \varphi \cot \frac{\gamma}{2} \right) \tag{6.29}$$

undisturbed gas flow

$$\ell_i = \frac{2 B_i L}{b_0} \tag{6.30}$$

hydrodynamic equations

$$0 = \mu_p \left(\frac{\partial 2}{\partial u_p} y \right) - \frac{\partial P_p}{\partial x} + g \varrho_p \sin \alpha, \tag{6.31}$$

$$\frac{\partial P_p}{\partial y} = 0, \qquad p = L, G \tag{6.32}$$

$$\frac{\partial p_L}{\partial x} = \frac{\partial p_L}{\partial y} = const = \Delta p \tag{6.33}$$

$$u_L|_{y=0} = 0 \qquad u_L|_{y=\delta} = u_G \tag{6.34}$$

Todo list